SELF-CONSISTENT TREATMENT

of

ELECTRON PROPAGATION IN DEVICES

M. Cahay, M. McLennan, S. Bandyopadhyay
S. Datta and M.S. Lundstrom

School of Electrical Engineering
Purdue University
W. Lafayette, IN USA 47907

ABSTRACT

The modeling of collisionless electron propagation in devices with a self-consistent treatment of the electrostatic potential is discussed. A technique for iteratively solving the wave equation along with Poisson's equation is presented, and factors affecting convergence of the solution are discussed. The importance of the self-consistent potential is illustrated by example computations for resonant tunneling structures. Finally, extensions of the technique to treat more realistic band structures and carrier scattering are discussed.

1. INTRODUCTION

Classical device analysis and simulation techniques are becoming increasingly questionable as device dimensions shrink and become comparable to a DeBroglie wavelength (typically 100 Å to 1000 Å). Several devices whose operation is based on quantum interference have been proposed and demonstrated [1-7]. New device modeling approaches, which explicitly treat the wave nature of carriers will be required in order to simulate these devices and to assess the importance of quantum effects in ultra-small conventional devices. Future modeling techniques will treat electrons as waves propagating through the device according to Schrodinger's equation. Although several formalisms are being developed [8,9,10,11], a completely general, computationally feasible description of quantum transport in devices has not yet emerged. Simple treatments of quantum transport are useful for the insight into device performance that they can provide. They are

especially useful if a clear path is identified by which the restrictions of the simple model may be removed.

The purpose of this paper is to discuss the application of a technique pioneered by Tsu and Esaki [1,2] to the modeling of devices. We have extended this technique, which neglects carrier scattering, to evaluate the electron density *self-consistently* with the electrostatic potential. The basic technique is described in Sec. 2. and the self-consistent calculations in Sec. 3. Two major limitations of this model, the assumption of a simple band structure and the neglect of scattering, are discussed in Sec. 4 in which we describe our thoughts on how to relax these limitations and report on recent work in this area.

2. COLLISIONLESS ELECTRON PROPAGATION IN DEVICES

The technique used is briefly described as follows. Each of the two contacts of the one-dimensional device sketched in Fig. 1 is assumed to be in local thermodynamic equilibrium. The Fermi-levels of these contacts are separated by the applied bias. The contacts launch electrons into the device with a spectrum of wave-vectors, $\vec{k}$. The electron wavefunction in the device,

$$\Psi(\vec{r}) = \psi(x)\exp(i\vec{k}_t\cdot\vec{r}_t)\,, \qquad (1)$$

is determined by solving

$$\frac{d}{dx}\left[\frac{1}{\gamma(x)}\frac{d\psi(x)}{dx}\right] = \frac{2m^*(x_C)}{\hbar^2}\left[E_p + E_t(1-\gamma(x)^{-1}) - E_C(x)\right]\psi(x) = 0 \qquad (2)$$

for the envelope function $\psi(x)$. In (2) $\gamma(x) = m^*(x)/m^*(x_C)$ describes the spatial variation of the effective mass with respect to that in the contact $m^*(x_C)$. E_t is the transverse energy, $\hbar^2k_t^2/2m^*(x_C)$, and E_p the longitudinal energy, $\hbar^2k_x^2/2m^*(x_C)$. The contact is located at $x = x_C$.

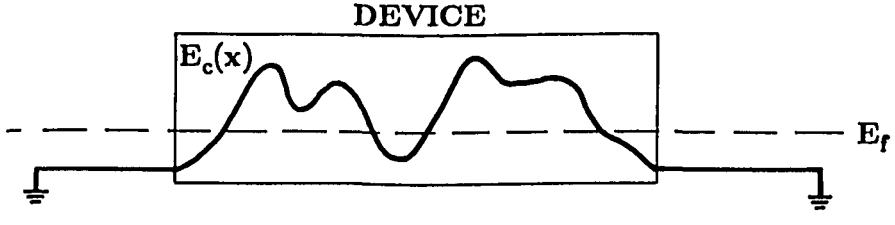

Fig. 1 One dimensional device structure.

The electron density is obtained by summing the contributions due to the various $\vec{k}$ for each of the two oppositely flowing currents. For electrons impinging from the left, we have

$$n^{l-r}(x) = \frac{1}{4\pi^3}\int d^3\vec{k} \left| \psi_{k_x}{}^{+}(x) \right|^2 f(E_k) , \qquad (3)$$

where $f(E_k)$ is the Fermi-Dirac factor with the Fermi level of the left contact.

When $m^*(x)$ is position-independent, $\psi(x)$ as determined from (2) is independent of $\vec{k}_t$ and the integral over k_y and k_z in (3) can be performed analytically. The result is

$$n^{l-r}(x) = \frac{1}{2\pi}\int_0^\infty dk_x \left| \psi_{k_x}{}^{+}(x) \right|^2 \sigma(k_x) \qquad (4)$$

where $\sigma(k_x)$ is given by

$$\sigma(k_x) = \frac{m^*(x_C)\, k_B T}{\pi\hbar^2} \ln\left[1 + \exp((E_{FL} - E_{CL} - E_p)/k_B T)\right], \qquad (5)$$

where $E_p = \hbar^2 k_x{}^2/2m^*(x_C)$ and E_{FL} is the Fermi level in the left contact. The total electron density versus position is then obtained by adding the contribution of the left contact to that of the right.

An examination of (2) shows that $\psi(x)$ depends on the transverse energy when the effective mass varies with position. The result is that the integral over k_x and k_y cannot be performed analytically and a rigorous evaluation of $n(x)$ would require a calculation of $\psi(x)$ over a grid of transverse energies. To avoid this complication, we follow Vassell [9] and replace E_t in (2) by its thermal average $k_B T$.

The computational procedure consists of incrementing the longitudinal wave-vector from zero to some maximum value. For each wave-vector, the wavefunction is computed, and the contribution to $n(x)$ for electrons between k_x and $k_x + dk_x$ is evaluated. The contributions for each k_x are then summed to evaluate the integral (4) numerically. This procedure is then repeated for the other contact.

To calculate $\psi(x)$, consider two sets of plane waves, one impinging from the left and the other one from the right (see Fig. 1) one can then in principle calculate the shape of the wave function inside the device for any value of the incident wave vector k_x. For an arbitrary potential within the device, this problem cannot be solved analytically, but from a numerical point of view, the potential may be approximated by a finite number of steps as depicted in Fig. 2. At each interface, continuity of the current requires continuity of $\psi(x)$ and $\frac{1}{m^*(x)}\, d\psi/dx$. There are numerous ways to solve for $\psi(x)$ among them the technique of cascading transfer matrices which is discussed in references [1] and [2].

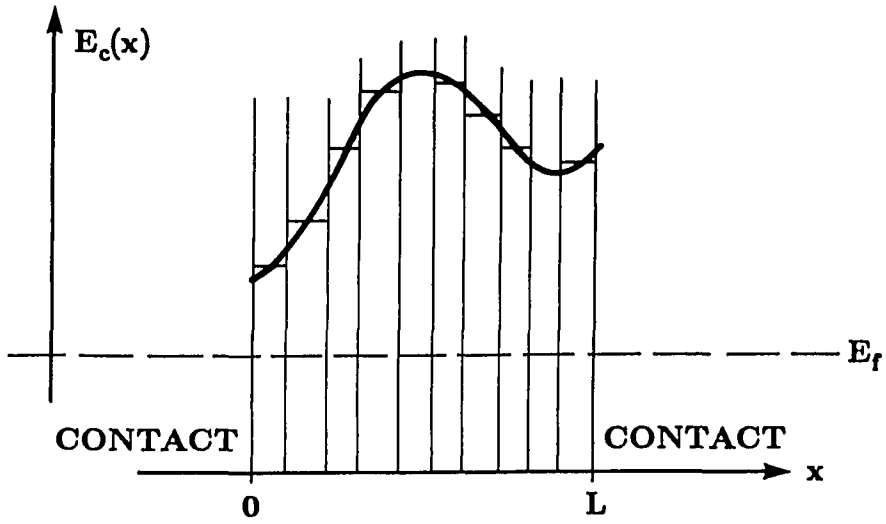

Fig. 2 The assumed $E_C(x)$ for numerical computations.

A simple recursive solution of the wave equation has also proved successful [12]. Referring to Fig. 2, we write the solution in the section to the left of node j as

$$\psi_j = F_j e^{ik_j x} + R_j e^{-ik_j x} \quad , \tag{6}$$

where

$$k_j = \sqrt{\frac{2m^*(x_C)}{\hbar^2}\left[E_p + E_t(1-\gamma_j^{-1}) - E_{Cj}\right]} \tag{7}$$

is the wavevector in the jth section. Applying the boundary conditions at node j we find

$$F_j e^{ik_j x_j} + R_j e^{-ik_j x_j} = F_{j+1} e^{ik_{j+1} x_j} + R_{j+1} e^{-ik_{j+1} x_j} \quad , \tag{8}$$

and

$$\frac{k_j}{\gamma_j}\left[F_j e^{ik_j x_j} - R_j e^{-ik_j x_j}\right] = \frac{k_{j+1}}{\gamma_{j+1}}\left[F_{j+1} e^{ik_{j+1} x_j} - R_{j+1} e^{-ik_{j+1} x_j}\right]. \quad (9)$$

Equations (8) and (9) may be solved for

$$\phi_j{}^t = \frac{1}{2}\left(1 + \frac{k_{j+1}\,\gamma_j}{k_j\,\gamma_{j+1}}\right) e^{-i\delta_{j+1}}\,\phi_{j+1}{}^t + \frac{1}{2}\left(1 - \frac{k_{j+1}\,\gamma_j}{k_j\,\gamma_{j+1}}\right) e^{i\delta_{j+1}}\,\phi_{j+1}{}^r \quad (10)$$

and

$$\phi_j{}^r = \frac{1}{2}\left(1 - \frac{k_{j+1}\,\gamma_j}{k_j\,\gamma_{j+1}}\right) e^{-i\delta_{j+1}}\,\phi_{j+1}{}^t + \frac{1}{2}\left(1 + \frac{k_{j+1}\,\gamma_j}{k_j\,\gamma_{j+1}}\right) e^{i\delta_{j+1}}\,\phi_{j+1}{}^r \quad (11)$$

where

$$\delta_j = k_j(x_j - x_{j-1}) \quad (12)$$

is the complex phase thickness and

$$\phi_j{}^t = F_j e^{ik_j x_j} \quad (13)$$

and

$$\phi_j{}^r = R_j e^{-ik_j x_j}. \quad (14)$$

For electron waves launched from the left contact, we assume $\phi_{N+1}{}^t = 1$ and $\phi_{N+1}{}^r = 0$; Equations (10) and (11) then enable us to calculate $\psi_j = \phi_j{}^t + \phi_j{}^r$ recursively from node N to 1.

To illustrate the technique, we present results for a simple resonant tunneling structure (similar to that reported in [4]) whose conduction band edge versus position is shown in Fig. 3. The computed n(x) with this *assumed* $E_C(x)$ is plotted in Fig. 4. These results were obtained with a spatial grid of 140 nodes and a grid with 1000 nodes in k_x-space. It should be stressed that the computed n(x) implies that a substantial space-charge exists and, therefore, the assumed $E_C(x)$ cannot be correct. Accurate evaluations of the energy band and carrier density profiles in this structure require a *self-consistent* solution of the wave equation with Poisson's equation as discussed in the following section.

3. SELF-CONSISTENT TREATMENT OF ELECTRON PROPAGATION

The techniques discussed in the previous section permit one to evaluate the electron charge density n(x) and the current voltage characterisitics if the conduction band profile is *assumed* to be known. For resonant tunneling devices, the electrons spend a great deal of time trapped between confining barriers and the electron density may be large. For such cases, the energy band profile

$$E_C(x) = E_o - \chi(x) - qV(x), \quad (15)$$

must be evaluated self-consistently. In (15), E_o is the field-free vacuum level, $\chi(x)$ the electron affinity, and V(x) the electrostatic potential. The electrostatic potential is obtained from Poisson's equation

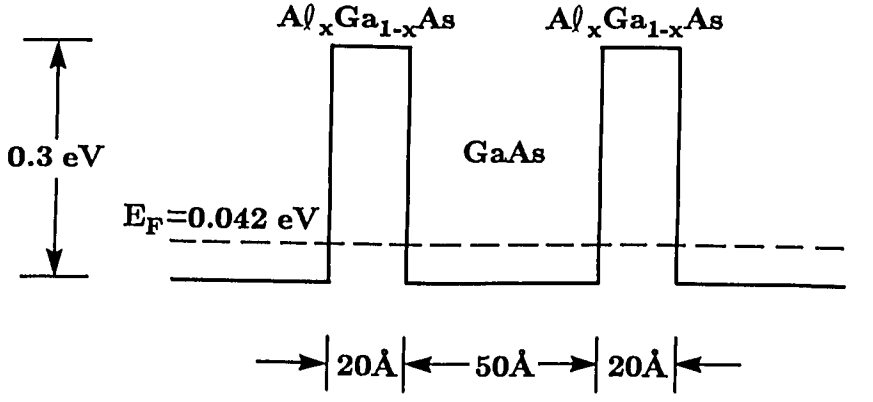

Fig. 3 Device structure and dimensions for the resonant tunneling example.

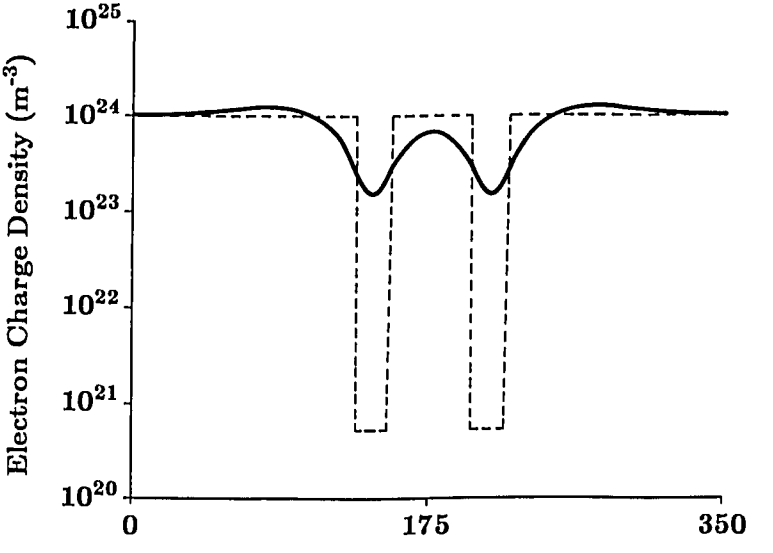

Fig. 4 Computed electron density in the resonant tunneling example with an assumed, flat conduction band profile. The classical carrier density, also assuming a flat conduction band profile, is shown dashed.

$$\frac{d}{dx}\left[\epsilon_S(x)\,\frac{dV(x)}{dx}\right] = -q\left[\,N_D^+(x) - N_A^+(x) - n(x)\,\right], \qquad (16)$$

where the carrier density n(x) is obtained by solving the wave equation as described in Sec. 3.

The procedure for modeling the propagation of electrons in semiconductor microstructures self-consistently is as follows. One first assumes an electrostatic potential V(x). The wave equation is then solved for $\psi(x)$ and n(x) is evaluated from (4). With this n(x), Poisson's equation is solved for a new V(x). The new V(x) is used to update $E_C(x)$ which is inserted in the wave equation to solve for an updated n(x). The process is repeated until V(x) converges. We currently use V(x) as calculated classically for the microstrure [11] as the initial guess for the iteration; Poisson's equation is solved by a finite difference technique.

To illustrate the self-consistent calculations, we consider the same resonant tunneling structure discussed in Sec. 2. Figure 5 compares $E_C(x)$ computed self-consistently with that assumed in Sec. 2. This figure shows that space-charge effects substantially lower the energy band profile in the well. If the depth of this well is sufficient, a bound state may occur - in which case we should add to (3) the charge density associated with electrons in this well. For the structure considered, no such bound state occurs.

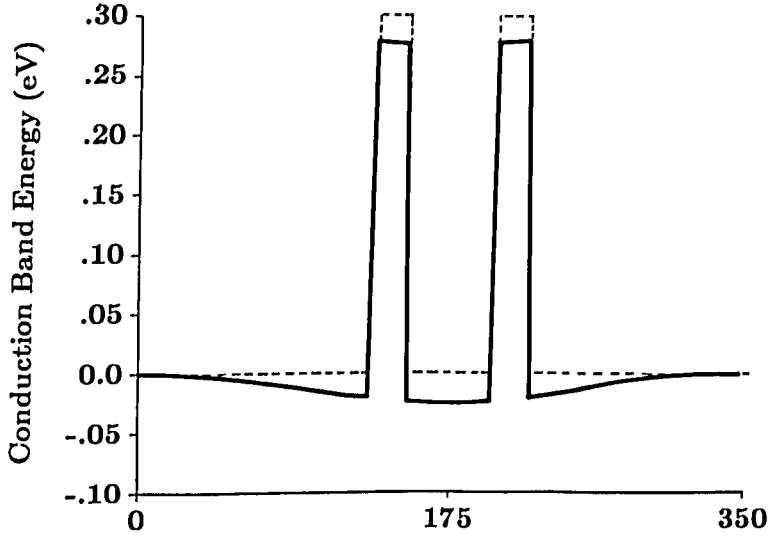

Fig. 5 Computed self-consistent energy band profile for the resonant tunneling example (solid line) compared with the assumed energy band profile used in Sec. 2 (dashed line).

Obtaining convergence in the self-consistent calculations requires some care. Such convergence problems may be especially difficult for resonant tunneling structures. The difficulties are best explained with the aid of Fig. 6 which shows the contributions to n(x) from electrons impinging from the left contact for various x and k_x. (A similar plot exists for electrons entering from the right contact.) For each x, the contributions in the plot must be summed over k_x to find n(x). Resonant tunneling produces sharp peaks in k_x space which must be accurately resolved to evaluate n(x). The problem is especially severe when the confining barriers are wide. As the iteration proceeds, the location in k_x space of the peaks changes as $E_C(x)$ changes. Unless the peaks are accurately resolved, the iteration does not converge. When a suitable k_x–space grid is chosen, the calculations converge rapidly as Fig. 7 shows.

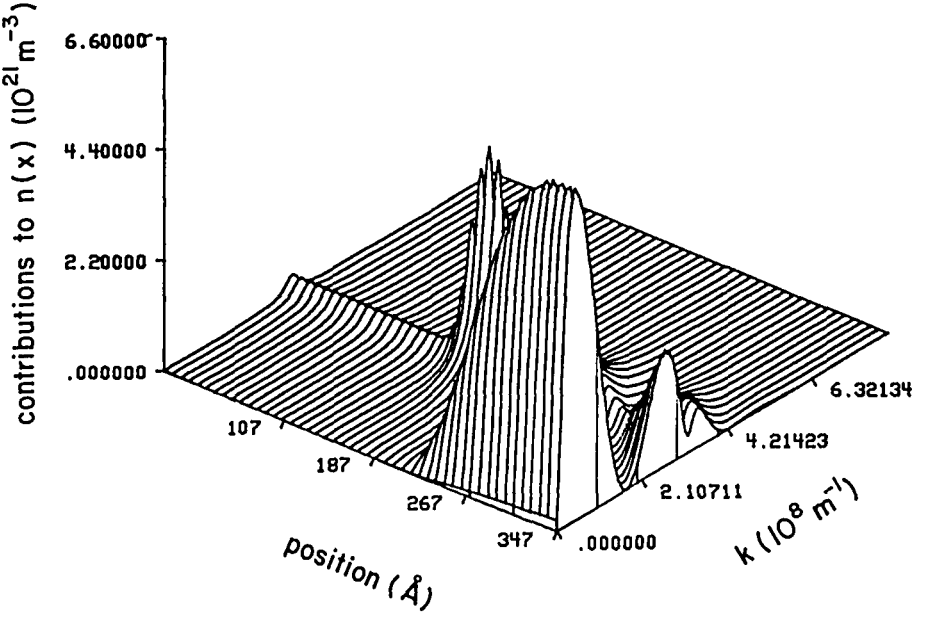

Fig. 6 Contribution to n(x) versus k_x and position, x.

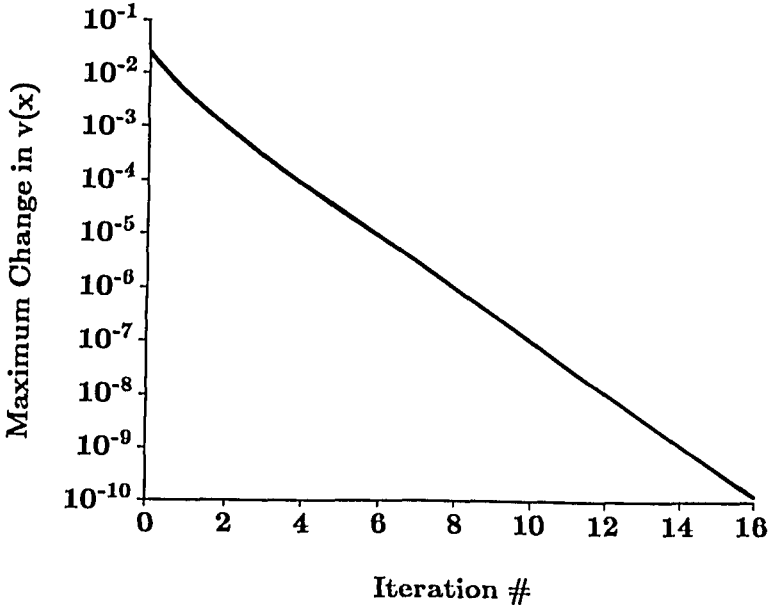

Fig. 7 Maximum change in electrostatic potential versus iteration for the resonant tunneling example.

4. SUMMARY

In this paper we presented a technique for self-consistently computing the electron density and current in semiconductor microstructures which are short enough to neglect scattering. Example computations illustrated the importance of the self-consistent potential. Several authors have previously treated the propagation of electrons in microstructures without considering the self-consistent potential - others have treated bound states self-consistently. Our work differs in its emphasis on the self-consistent treatment of propagating waves. A key limitation of the approach is its neglect of scattering which will be present to some extent in any realistic device. An approach which appears to hold promise for incorporating scattering within the basic -Esaki approach consists of the Monte Carlo solution of the wave equation as opposed to the deterministic solution outlined in Sec. 2.

Acknowledgement - This work was supported by the Semiconductor Research Corporation, Contract 83-01-001 and by the National Science Foundation.

REFERENCES

[1] TSU, R. and ESAKI, L., Appl. Phys. Lett., Vol. 22, pp. 562-564, 1973.

[2] CHANG, L.L., ESAKI, L., and TSU, R., Appl. Phys. Lett., Vol. 47, pp. 415-417, 1985.

[3] SOLNER, T.G., et al., Appl. Phys. Lett., Vol. 43, pp. 588-590, 1983.

[4] SEWCHUK, T.J., et al., Appl. Phys. Lett., Vol. 46, pp. 508-510, 1985.

[5] MENDEZ, E.E., et al., Appl. Phys. Lett., Vol. 24, pp. 593-595, 1974.

[6] KIRCHOEFER, S.W., et al., Appl. Phys. Lett., Vol. 46, pp. 855-857, 1985.

[7] DATTA, S., et al., Phys. Rev. Lett., Vol. 21, pp. 2344-2347, 1985.

[8] BARKER, T.R. and FERRY, D.K., Solid-State Electron., Vol. 23, 519, (1980).

[9] VASSEL, M.O., et al., J. Appl. Phys., Vol. 54, pp. 5206-5213, 1983.

[10] FRENSLEY, W.R., J. Vac. Science Tech., Vol B3, p. 1261, 1985.

[11] GRAY, J.L. and LUNDSTROM, M.S., IEEE Trans. Electron Dev., Vol. ED-32, pp. 2102-2109, 1985.

[12] KOLTUN, M.M., *Selective Optical Surfaces for Solar Energy Converters,* Allerton Press, New York, 1981.